

AperTO - Archivio Istituzionale Open Access dell'Università di Torino

## Soil networks become more connected and take up more carbon as nature restoration progresses

**This is a pre print version of the following article:**

*Original Citation:*

*Availability:*

This version is available <http://hdl.handle.net/2318/1622913> since 2017-05-15T15:35:32Z

*Published version:*

DOI:10.1038/ncomms14349

*Terms of use:*

Open Access

Anyone can freely access the full text of works made available as "Open Access". Works made available under a Creative Commons license can be used according to the terms and conditions of said license. Use of all other works requires consent of the right holder (author or publisher) if not exempted from copyright protection by the applicable law.

(Article begins on next page)

## **Soil networks become more connected and take up more carbon as nature restoration progresses**

**Authors:** Elly Morriën<sup>1,2†</sup>, S. Emilia Hannula<sup>3†</sup>, L. Basten Snoek<sup>1,5</sup>, Nico R. Helmsing<sup>4</sup>, Hans Zweers<sup>3</sup>, Mattias de Hollander<sup>3</sup>, Raquel Luján Soto<sup>1</sup>, Marie-Lara Bouffaud<sup>6</sup>, Marc Buée<sup>8,9</sup>, Wim Dimmers<sup>10</sup>, Henk Duyts<sup>1</sup>, Stefan Geisen<sup>1,11</sup>, Mariangela Girlanda<sup>12,13</sup>, Rob I. Griffiths<sup>14</sup>, Helene-Bracht Jørgensen<sup>15</sup>, John Jensen<sup>16</sup>, Pierre Plassart<sup>6</sup>, Dirk Redecker<sup>7</sup>, Rüdiger M. Schmelz<sup>17,18</sup>, Olaf Schmidt<sup>19,20</sup>, Bruce C. Thomson<sup>14</sup>, Emilie Tisserant<sup>8,9</sup>, Stephane Uroz<sup>8,9</sup>, Anne Winding<sup>21</sup>, Mark J. Bailey<sup>14</sup>, Michael Bonkowski<sup>11</sup>, Jack H. Faber<sup>10</sup>, Francis Martin<sup>8,9</sup>, Philippe Lemanceau<sup>6</sup>, Wietse de Boer<sup>3,22</sup>, Johannes A. van Veen<sup>3,23</sup>, Wim H. van der Putten<sup>1,5</sup>

### **Affiliations:**

<sup>1</sup>NIOO-KNAW, Terrestrial Ecology, Droevendaalsesteeg 10, 6708 PB, Wageningen, The Netherlands.

<sup>2</sup>Institute for Biodiversity and Ecosystem Dynamics, Earth Surface Sciences Group (IBED-ESS), University of Amsterdam, P.O. Box 94246, 1090 GE, Amsterdam, The Netherlands.

<sup>3</sup>NIOO-KNAW, Microbial Ecology, Droevendaalsesteeg 10, 6708 PB, Wageningen, The Netherlands.

<sup>4</sup>NIOO-KNAW, Aquatic Ecology, Droevendaalsesteeg 10, 6708 PB, Wageningen, The Netherlands.

<sup>5</sup>Wageningen University, Laboratory of Nematology, Droevendaalsesteeg 1, 6708 PB, Wageningen, The Netherlands.

<sup>6</sup>INRA, UMR 1347 Agroécologie, 17 rue Sully, BV 68510, F-21065 Dijon Cedex, France.

<sup>7</sup>Université de Bourgogne, UMR 1347 Agroécologie, 17 rue Sully, BV 68510, F-21065 Dijon Cedex, France.

<sup>8</sup>INRA, UMR 1136 “Interactions Arbres Micro-organismes”, Centre INRA de Nancy, F-54280 Champenoux, France.

<sup>9</sup>Université de Lorraine, UMR 1136 “Interactions Arbres Micro-organismes” F-54000 Vandoeuvre-les-Nancy, France.

<sup>10</sup>Alterra Wageningen UR, Droevendaalsesteeg 3, P.O. Box 47, 6700 AA, Wageningen, The Netherlands.

<sup>11</sup>University of Cologne, Institute of Zoology, Department of Terrestrial Ecology, Zùlpicher Str 47b, 50674 Cologne, Germany.

<sup>12</sup>University of Torino, Dept. Scienze della Vita e Biologia dei Sistemi, Viale Mattioli 25, 10125 Torino, Italy.

<sup>13</sup>National Research Council, Istituto per la Protezione Sostenibile delle Piante (IPSP-CNR), Viale Mattioli 25, 10125 Torino, Italy

<sup>14</sup>NERC Centre for Ecology & Hydrology, Wallingford, Oxford, UK.

<sup>15</sup>Lund University, Department of Biology, SE-22362, Sweden.

<sup>16</sup>Dep. of Bioscience, Aarhus University, Vejlsvøvej 25, 8600 Silkeborg, Denmark.

<sup>17</sup>ECT Oekotoxikologie GmbH, Böttgerstr. 2-14, 65439 Flörsheim, Germany

<sup>18</sup>Universidad de A Coruña, Science Faculty, Department of Animal Biology, Plant Biology and Ecology, Rua da Fraga 1, 15008 A Coruña, Spain.

<sup>19</sup>UCD School of Agriculture and Food Science, University College Dublin, Dublin 4, Ireland.

<sup>20</sup>UCD Earth Institute, University College Dublin, Dublin 4, Ireland.

<sup>21</sup>Dep. Environmental Science, Aarhus University, Frederiksborgvej 399, PO Box 358, 4000 Roskilde, Denmark.

<sup>22</sup>Wageningen University, Department of Soil Quality, PO Box 47, 6700AA Wageningen, the Netherlands.

<sup>23</sup>Leiden University, Department of Plant Ecology and Phytochemistry, P.O. Box 9505, 2300 RA Leiden, The Netherlands.

† Both authors contributed equally to the work

**Soil organisms play an important role in aboveground community dynamics and ecosystem functioning in both natural and disturbed ecosystems<sup>1</sup>. However, most studies have focussed on black box approaches or on specific groups of soil biota<sup>2</sup>, whereas little is known about entire soil networks. Here, we show that during the course of nature restoration on abandoned arable land a compositional shift in soil microbiota, preceded by tightening of the belowground networks, corresponds with enhanced efficiency of carbon uptake. In mid and long-term abandoned field soil, carbon uptake by fungi increases without an increase in fungal biomass or shift in bacterial to fungal ratio. The implication of our findings is that during nature restoration the efficiency of nutrient cycling and carbon uptake can increase by a shift in fungal composition and/or fungal activity without an increase in fungal to bacterial biomass ratio. Therefore, we propose that relationships between soil food web structure and carbon cycling in soils need to be reconsidered.**

**Keywords:** Belowground biodiversity-Ecosystem functioning-Soil community structure-Network topology-Soil cores-Stable isotopes

**One Sentence Summary:** Changes in the belowground community composition and tightening in the co-occurring network of soil biota lead to enhanced efficiency of carbon uptake during nature restoration on ex-arable land.

## **Main Text:**

Many ecosystems worldwide face exposure to intensified human use<sup>3-5</sup>, which has resulted in loss of biodiversity<sup>6</sup>, altered functioning, and altered provisioning of ecosystem services<sup>7</sup>. The abandonment of disturbed land represents one of the most widely used restoration strategies implemented at a global scale<sup>18</sup>, with the potential to promote biodiversity, and associated ecosystem services. However, the restoration of natural ecosystem functioning and

soil properties is known to be a long-term process<sup>8,9</sup>, dependent upon the time it takes to restore connections between different components of the community<sup>10</sup>. Over half a century ago, Odum identified mechanistic linkages between the successional dynamics of natural communities and the functioning of natural ecosystems. Specifically, as communities progress through succession, diversity is expected to increase and nutrients will become 'locked-up' in the biota, with consequences for the build-up of soil organic matter and closure of the mineral cycles<sup>11</sup>. More recently, the interplay between aboveground and belowground biodiversity has emerged as a prominent determinant of the successional dynamics in biological communities<sup>12</sup>. However, little is known about how changes in the soil biota contribute to the associated changes in ecosystem functioning.

In ecosystems undergoing secondary succession, it is evident that available nitrogen diminishes, primary productivity decreases, and the plant community shifts from fast- to slow-growing plant species<sup>1</sup>. There is less evidence of an increase of soil biodiversity<sup>13</sup>, and evidence of a relationship between soil biodiversity and ecosystem functioning is mixed, at best<sup>2,14-16</sup>. As a result, it is still unclear how soil and plant community composition relate to each other and what is the relative role of plants and soil biota in driving soil processes and plant community development<sup>17,18</sup>.

Interestingly, studies on a time series (chronosequence) of abandoned arable fields revealed that carbon and nitrogen mineralization by the soil food web increases during secondary succession<sup>19</sup>. This implies a more active soil microbial community in later successional stages<sup>20-22</sup> where bacterial-dominated systems are expected to be replaced by fungal-dominated systems<sup>23</sup> with more carbon turnover via fungi<sup>24</sup> and their consumers<sup>25</sup>. However, data to test these assumptions are largely lacking. Therefore, the aim of the present study was to examine how biodiversity, composition, and structure of the soil community change during successional development of restored ecosystems. We used a well-established chronosequence of nature restoration sites on ex-arable lands that represent over 30 years of nature restoration. We determined biodiversity of almost all taxonomic groups of soil biota, analysed their network structure, and added labelled carbon dioxide and mineral nitrogen to intact plant-soil systems in order to track their uptake by the soil food web. We tested the hypothesis that functional changes in carbon and nitrogen flows relate more strongly to the belowground community network structure than to belowground biodiversity.

## Results (?)

In 2011, we collected soil samples from nine natural grasslands that have been abandoned 6-31 years ago, all situated on the same parent soil material. Three replicate grasslands were recently abandoned, three mid-term, and three long-term (Supplementary Fig 1, Supplementary Table 1). Bacteria, Archaea and fungi were identified by molecular techniques, whereas protists, nematodes, micro-arthropods, enchytraeids and earthworms were extracted and identified morphologically (See Methods for details). From the 10,395 taxa identified from the nine grasslands, 3,553 species remained for the network analyses after removal of single occurrences from each of the abandonment stages (Supplementary Tables 2&3 and Supplementary Fig. 2). For each grassland abiotic soil properties were measured, species data were recorded, and statistical analyses made (Supplementary Figs. 3, 4&5, Supplementary Tables 4&5). We created a Spearman-rank correlation matrix based on abundance data of species and visualized the correlation matrix as a network considering species as functional and taxonomic groups, respectively.

We tested functional consequences of altered network structures by stable isotope probing applying dual labelled ammonium nitrate ( $^{15}\text{NH}_4^{15}\text{NO}_3$ ) to the soil, and  $^{13}\text{CO}_2$  to the plants in 90 intact soil cores that were collected from the same 9 grasslands that were used for the soil network analysis. Soil cores were collected from sites within the 9 grasslands that were all dominated by the same three plant species (Supplementary Figs. 6&7). The carbon and nitrogen uptake by different species groups and trophic levels of the soil food webs was resolved by isotopic measurements of the microbes identified based upon lipid biomarkers, and of soil fauna identified by morphology into aggregated groups according to the network analysis (Supplementary Table 3).

During the course of succession following land abandonment, there was an increase in the number of strong correlations between groups of soil organisms based on species abundance data with Spearman-rank correlation  $>0.9$  (Fig. 1A, Supplementary Table 6). We consider strong correlations as network tightening, which we define as a 'significant increase in percentage connectance, and an increase in the strong correlations as a percentage of all possible correlations'. Network structure change was the most pronounced between recently and mid-term abandoned fields, largely due to increased correlations between bacteria and fungi (Fig. 1B, Supplementary Table 6). Analysis of co-occurrence showed that patterns in network structure were robust for the type of comparison; network analysis using presence-absence data in the correlation matrix showed the same transition in network tightening between recent and mid-term abandonment stages (Supplementary Figs. 8&9).

During succession the numbers of plant species declined (Supplementary Fig. 4 and Supplementary Table 5, respectively), plant species composition changed, and plant community structure became less even, as is indicated by reduced H-value in the longer-term abandoned fields (Supplementary Fig. 5, Supplementary Table 7). Variation in abiotic soil properties was significantly higher in the recently abandoned fields than in the mid-term abandoned fields, however, there was no significant difference between variation in recent versus long-term abandoned fields (Supplementary Fig. 10). Abiotic conditions explained a substantial amount of variation of the different groups of soil biota (Supplementary Table 4). However, the increased network tightening from recent to long-term abandoned fields could not be explained by significantly declined variation in abiotic conditions.

The number of taxa in bacteria and most fungi showed a hump-shaped pattern, whereas numbers of taxa of arbuscular mycorrhizal fungi (AMF) significantly increased with progressing succession (Supplementary Fig. 4, Supplementary Table 5). The number of taxa of fungivorous cryptostigmatic mites, predaceous mesostigmatic mites, root-feeding nematodes, and bacterivorous nematodes in general also increased during the course of succession, whereas other species groups did not show any successional change at all (Supplementary Fig. 4, Supplementary Table 5). On the other hand, there were significant changes in soil community composition, amongst others in composition of bacteria, fungi, and their predators (Supplementary Table 7). Therefore, increased network tightening could not be explained only by a general convergence in plant community composition or soil properties, or by the total amount of soil biodiversity, whereas a contribution of changed composition of the soil community could not be excluded.

Analysis of  $^{13}\text{C}$  revealed that the tightening of the belowground networks coincided with increased efficiency of carbon uptake: in later successional stages that had been abandoned longer time ago, plants tended to have least newly photosynthesized carbon in their roots, whereas consumers, such as root-feeding nematodes and soil fungi contained most of the

supplied label (Fig. 2). This pattern becomes even clearer when considering the relative amounts of carbon in the microbes 1 day after pulse labelling (PLFA: Bacteria  $F_{2,13}=6.51$ ,  $p=0.01$ , Fungi  $F_{2,13}=2.85$ ,  $p=0.09$ , NLFA: AMF  $F_{2,13}=1.16$ ,  $p=0.34$ ) and, later, in consumers and their predators (Fig. 3). In the recently abandoned grasslands, fungi took up half of the carbon, whereas in long-term abandoned grasslands three quarters of the carbon was taken up by fungi. These changes could not be explained by increased fungal biomass, or by an increase in fungal to bacterial biomass ratio (Fig. 2 and Supplementary Fig. 11, respectively). The changes, however, go along with substantial shifts in microbial consumers. The combination of tighter connections and stronger labelling of the fungal channel in the mid and longer-term abandoned fields make us conclude that network tightening contributes to enhanced efficiency of carbon uptake by the soil food web.

In early successional stages at recently abandoned fields, fungivorous collembola and nematodes were the predominant fungal consumers, whereas in later succession stages mites took a larger proportion of the labelled carbon (Fig. 3). Interestingly, these differences in soil community functioning were recorded in spite of soil cores being collected from sites along the chronosequence that were largely dominated by the same three plant species (Supplementary Fig. 6). Therefore, our results suggest that successional changes in soil community structure and functioning can arise even under the same plant community composition. Such field-based evidence on the role of whole soil biodiversity in ecosystem functioning is quite rare<sup>16,2</sup>. Detailed analysis of incorporation of label into the soil food web revealed similar temporal patterns of incorporation of  $^{13}\text{C}$  and  $^{15}\text{N}$  into higher trophic levels. It is possible to analyse  $^{15}\text{N}$  in microbes, but methods do not allow distinguishing bacterial from fungal  $^{15}\text{N}$ . Therefore, we chose not to relate tightening of the belowground networks to the microbial efficiency of nitrogen use by the belowground food web (Supplementary Table 8, Supplementary Table 9 & Supplementary Fig. 12).

## Discussion (?)

The novel combination of correlation-based network analysis and isotope labelling shows that during land abandonment soil networks become more tight and that efficiency of the carbon uptake in the fungal channel of the soil food web increases, without an increase in the total amount of soil biodiversity, or in fungal to bacterial biomass ratios. For nitrogen, the non-microbial species groups revealed a similar pattern as for carbon. Tightening of the networks reflects stronger co-occurring patterns of variation in soil biota<sup>26</sup>. Increased carbon and nitrogen uptake capacity by the fungal channel in the soil food web can be explained by stronger co-occurrence of preys and their predators<sup>25</sup>, which enhances the efficiency of resource transfer in the soil food web compared to a soil food web where preys and predators are spatially isolated.

Increased network tightening may be due to several factors. First, tightening may be caused by successional shifts in species<sup>27</sup>. Bacteria and fungi showed hump-shaped development in numbers of taxa, whereas numbers of AMF taxa steadily increased, indirectly suggesting that there are indeed shifts in species composition along the successional gradient. AMF have been suggested to increasingly influence plant community composition with increasing time since land abandonment<sup>28</sup>. However, in our study network tightening is due to changes in more species groups than AMF alone. Second, increased tightening could be due to declined nutrient availability in the soil along the successional gradient<sup>19,29-30</sup>, which may enhance the necessity of stronger cooperative and trophic interactions between functional groups of soil biota.

Third, changes in the soil physical conditions can influence network tightening<sup>31</sup>. Arable soils are assumed to be relatively heterogeneous<sup>32,33</sup>, whereas natural succession following land abandonment will increase spatial heterogeneity in abiotic soil conditions<sup>34</sup>. Soil biota have a variety of responses to soil heterogeneity<sup>35</sup>. Increased soil heterogeneity could contribute to network tightening, when it enhances co-occurrence patterns of variation in the soil biota. We found reduced variation in soil abiotic properties from recent to mid-term abandoned fields, but there were no differences in variation between recent and longer-term abandonment stages, which only partly supports the possibility that changes in soil abiotic factors enhance network tightening. Further correlative analyses of soil abiotic properties and network tightening would require independent pairs, however, we do not have individual networks for each individual soil sample used for abiotic analyses.

Our <sup>13</sup>C/<sup>15</sup>N analyses revealed that a plant community dominated by the same species allocated less carbon and nitrogen to the roots in soil with late (long-term abandoned) than in early successional (recently abandoned) soil communities, but that the mid-late successional soil communities were more efficient in carbon uptake. It may be that low abundant plant species<sup>36</sup> or conversion of soil abiotic properties have changed soil functioning, but our results also support the suggestion that changes in soil community structure may precede succession in plant communities<sup>17,18</sup>.

Opposite to expected, during successional transition the fungal biomass and the fungal to bacterial biomass ratios did not increase. Thus, nature restoration resulted in a transition in terms of belowground taxonomical composition and fungal productivity, but not in terms of fungal biomass. Interestingly, saprotrophic fungi represented only 0.06-0.08 of the fungal to bacterial ratio of the total microbial biomass in PLFA's, which is in accordance with previous estimates<sup>37</sup>, yet these fungi processed most of the carbon in later successional stages (Fig. 3)<sup>24</sup>. Such changes in soil community structure and functioning have been rarely considered in relation to nature restoration<sup>10</sup>. Often, restoration targets are focusing on aboveground biodiversity and the presence of rare or red list species, although it has been demonstrated that adding particular soil inocula can direct vegetation development towards particular target systems<sup>38</sup>.

We conclude that over successional time the connectance of species in the soil community increases, while carbon uptake becomes more efficient, even without major changes in species composition of the dominant plants. Our network approach combined with labeling study concerns a substantially different approach compared to previous soil food web modeling studies<sup>19,39</sup>, because it is based on actual community composition, whereas food web models are based on biomass of entire feeding groups. Our results suggest that transition in fungal composition can change element cycling and carbon uptake in soil without an increase in fungal biomass or fungal to bacterial biomass ratio. We propose that there is a need to verify these findings also in other chronosequences, and re-think how soil food web structure influences carbon cycling in soils.

[Please paste your Methods section here.]

Data availability statement

## References

- 1 Bardgett, R. D. & Wardle, D. A. *Aboveground- belowground linkages: Biotic interactions, ecosystem processes, and global change*. First edition (Oxford University Press, 2010).
- 2 Bardgett, R. D. & van der Putten, W. H. Belowground biodiversity and ecosystem functioning. *Nature* **515**, 505-511, doi:10.1038/nature13855 (2014).
- 3 Vitousek, P. M., Mooney, H. A., Lubchenco, J. & Melillo, J. M. Human domination of Earth's ecosystems. *Science* **277**, 494-499, doi:10.1126/science.277.5325.494 (1997).
- 4 Tilman, D., Cassman, K. G., Matson, P. A., Naylor, R. & Polasky, S. Agricultural sustainability and intensive production practices. *Nature* **418**, 671-677, doi:10.1038/nature01014 (2002).
- 5 Rockstrom, J. *et al.* A safe operating space for humanity. *Nature* **461**, 472-475 (2009).
- 6 Hooper, D. U. *et al.* Effects of biodiversity on ecosystem functioning: A consensus of current knowledge. *Ecol Monogr* **75**, 3-35, doi:10.1890/04-0922 (2005).
- 7 Potschin, M., Haines-Young, R., Fish, R. & Kerry Turner, R. *Routledge Handbook of Ecosystem Services*. (Routledge, 2016).
- 8 Knops, J. M. H. & Tilman, D. Dynamics of soil nitrogen and carbon accumulation for 61 years after agricultural abandonment. *Ecology* **81**, 88-98, doi:10.1890/0012-9658(2000)081[0088:dosnac]2.0.co;2 (2000).
- 9 McLauchlan, K. K., Hobbie, S. E. & Post, W. M. Conversion from agriculture to grassland builds soil organic matter on decadal timescales. *Ecol Appl* **16**, 143-153, doi:10.1890/04-1650 (2006).
- 10 Kardol, P. & Wardle, D. A. How understanding aboveground-belowground linkages can assist restoration ecology. *Trends Ecol Evol* **25**, 670-679, doi:10.1016/j.tree.2010.09.001 (2010).
- 11 Odum, E. P. Strategy of ecosystem development. *Science* **164**, 262-&, doi:10.1126/science.164.3877.262 (1969).
- 12 Walker, L. R., Walker, J. & Hobbs, R. J. *Linking restoration and ecological succession*. 190 (Springer, 2007).
- 13 Scheu, S. & Schulz, E. Secondary succession, soil formation and development of a diverse community of oribatids and saprophagous soil macro-invertebrates. *Biodivers Conserv* **5**, 235-250, doi:10.1007/bf00055833 (1996).
- 14 Hunt, H. W. & Wall, D. H. Modelling the effects of loss of soil biodiversity on ecosystem function. *Global Change Biology* **8**, 33-50, doi:10.1046/j.1365-2486.2002.00425.x (2002).
- 15 Setälä, H., Berg, M. P. & Jones, T. H. in *Biological Diversity and Function in Soils* (eds Bardgett, R. D., Usher, M. B. & Hopkins, D. W.) 236-249 (Cambridge Univ. Press, 2005).
- 16 Nielsen, U. N., Ayres, E., Wall, D. H. & Bardgett, R. D. Soil biodiversity and carbon cycling: a review and synthesis of studies examining diversity-function relationships. *Eur J Soil Sci* **62**, 105-116, doi:10.1111/j.1365-2389.2010.01314.x (2011).
- 17 Mahaming, A. R., Mills, A. A. S. & Adl, S. M. Soil community changes during secondary succession to naturalized grasslands. *Appl Soil Ecol* **41**, 137-147, doi:10.1016/j.apsoil.2008.11.003 (2009).
- 18 Harris, J. Soil microbial communities and restoration ecology: facilitators or followers? *Science* **325**, 573-574, doi:10.1126/science.1172975 (2009).



- 19 Holtkamp, R. *et al.* Modelling C and N mineralisation in soil food webs during secondary succession on ex-arable land. *Soil Biol Biochem* **43**, 251-260, doi:10.1016/j.soilbio.2010.10.004 (2011).
- 20 Moore, J. C. & Hunt, H. W. Resource compartmentation and the stability of real ecosystems. *Nature* **333**, 261-263, doi:10.1038/333261a0 (1988).
- 21 de Ruiter, P. C., van Veen, J. A., Moore, J. C., Brussaard, L. & Hunt, H. W. Calculation of nitrogen mineralization in soil food webs. *Plant Soil* **157**, 263-273 (1993).
- 22 Holtkamp, R. *et al.* Soil food web structure during ecosystem development after land abandonment. *Appl Soil Ecol* **39**, 23-34, doi:10.1016/j.apsoil.2007.11.002 (2008).
- 23 de Vries, F. T., Bloem, J., van Eekeren, N., Brusaard, L. & Hoffland, E. Fungal biomass in pastures increases with age and reduced N input. *Soil Biol Biochem* **39**, 1620-1630, doi:10.1016/j.soilbio.2007.01.013 (2007).
- 24 Clemmensen, K. E. *et al.* Roots and Associated Fungi Drive Long-Term Carbon Sequestration in Boreal Forest. *Science* **339**, 1615-1618, doi:10.1126/science.1231923 (2013).
- 25 Crowther, T. W. *et al.* Top-down control of soil fungal community composition by a globally distributed keystone consumer. *Ecology* **94**, 2518-2528, doi:10.1890/13-0197.1 (2013).
- 26 Barberán, A., Bates, S. T., Casamayor, E. O. & Fierer, N. Using network analysis to explore co-occurrence patterns in soil microbial communities. *ISME Journal* **6**, 343-351, doi:10.1038/ismej.2011.119 (2012).
- 27 Jaillard, B., Rapaport, A., Harmand, J., Brauman, A. & Nunan, N. Community assembly effects shape the biodiversity-ecosystem functioning relationships. *Funct Ecol* **28**, 1523-1533, doi:10.1111/1365-2435.12267 (2014).
- 28 Kardol, P., Bezemer, T. M. & van der Putten, W. H. Temporal variation in plant-soil feedback controls succession. *Ecol Lett* **9**, 1080-1088, doi:10.1111/j.1461-0248.2006.00953.x (2006).
- 29 Tilman, D. *Plant strategies and the dynamics and structure of plant communities*. (Princeton University Press, 1988).
- 30 Wardle, D. A. *et al.* Linking vegetation change, carbon sequestration and biodiversity: insights from island ecosystems in a long-term natural experiment. *J Ecol* **100**, 16-30, doi:10.1111/j.1365-2745.2011.01907.x (2012).
- 31 Olf, H. *et al.* Parallel ecological networks in ecosystems. *Philosophical Transactions of the Royal Society B-Biological Sciences* **364**, 1755-1779, doi:10.1098/rstb.2008.0222 (2009).
- 32 Robertson, G. P. & Freckman, D. W. The spatial distribution of nematode trophic groups across a cultivated ecosystem. *Ecology* **76**, 1425-1432, doi:10.2307/1938145 (1995).
- 33 Moll, J. *et al.* Spatial Distribution of Fungal Communities in an Arable Soil. *PLoS ONE* **11**, e0148130, doi:10.1371/journal.pone.0148130 (2016).
- 34 Fraterri, J. M., Turner, M. G., Pearson, S. M. & Dixon, P. Effects of past land use on spatial heterogeneity of soil nutrients in southern appalachian forests. *Ecol Monogr* **75**, 215-230, doi:10.1890/03-0475 (2005).
- 35 Ettema, C. H. & Wardle, D. A. Spatial soil ecology. *Trends Ecol Evol* **17**, 177-183, doi:10.1016/s0169-5347(02)02496-5 (2002).
- 36 De Deyn, G. B. *et al.* Additional carbon sequestration benefits of grassland diversity restoration. *J Appl Ecol* **48**, 600-608, doi:10.1111/j.1365-2664.2010.01925.x (2011).
- 37 Rousk, J. & Bååth, E. Growth of saprotrophic fungi and bacteria in soil. *FEMS Microbiol Ecol* **78**, 17-30, doi:10.1111/j.1574-6941.2011.01106.x (2011).

- 38 Wubs, E. R. J., Van der Putten, W. H., Bosch, M. & Bezemer, T. M. Soil inoculation steers restoration of terrestrial ecosystems. *Nature Plants*, doi:DOI: 10.1038/NPLANTS.2016.107 (2016).
- 39 de Vries, F. T. *et al.* Soil food web properties explain ecosystem services across European land use systems. *Proceedings of the National Academy of Sciences* **110**, 14296-14301, doi:10.1073/pnas.1305198110 (2013).

**Acknowledgments:** This study was carried out as part of the EcoFINDERS research project (EU-FP7-264465). We thank Rebecca Pas for processing labelled material, Eefje Sanders for extracting PLFAs and NLFAs and sorting enchytraeids, earthworms and spiders for the labelling experiment, Thomas Verschut for sorting labelled mites and collembolans, Javier Moliner Urdiales and Bekir Faydaci for collecting living soil-cores for the pulse labelling experiment, Agata Pijl, Valeria Bianciotto, Claudia Bragalini, Marine Peyret-Guzzon, Herbert Stockinger and Diederik van Tuinen for preparing libraries for pyrosequencing, Peter de Vries for drawing Supplementary Figure 1. The UMR1136 is supported by the ANR through the Laboratory of Excellence Arbre (ANR-11- LABX-0002-01). We thank George Kowalchuk, Peter de Ruiter, Thomas Crowther and Kelly Ramirez for their valuable comments on the manuscript. This is NIOO-KNAW publication xxxx.

**Authors contributions:** WHvdP and PL were involved in designing the field survey, EM, PP, WD, JHF, and WHvdP collected the soil samples for the network analyses. EM and SEH designed and performed the pulse labelling experiment, WdB and JAvV advised about the pulse labelling experiment, NRH performed the EA-IRMS analyses for the labelling experiment, HZ performed the GC-c-IRMS analyses for the pulse labelling experiment; LBS performed the network analyses, M-LB, MG, BCT, RIG, DR, MB, SU, FM, PP, and SEH were involved in the pyrosequencing of AMF, bacteria, archaea and fungi, MB, ET and MdH were involved in the bioinformatics, SG, MB and AW identified and analysed protozoa, HD identified- and RLS sorted labelled nematodes, H-BJ analysed PLFA's, RMS identified enchytraeids, WD mites, JJ collembolans, OS earthworms, and PP provided the environmental data. EM, SHE and LBS did the data analysis and statistics, EM, SEH and WHvdP wrote the manuscript; all others co-commented on the manuscript.

**Author information:** The sequencing data is stored in Sequence Read Archive (SRA) and can be found under accession numbers SRP049204 and SRP044011. Reprints and permissions information is available at [www.nature.com/reprints](http://www.nature.com/reprints). Correspondence and requests for materials should be addressed to EM ([e.morrien@nioo.knaw.nl](mailto:e.morrien@nioo.knaw.nl)).

## Supplementary:

Methods

References (40-92)

Supplementary Tables 1-9

Supplementary Figures 1-13

## Figure captions

### **Figure 1 Network visualisation of the interaction strengths between the species sub-groups (A) and main species groups (B) in semi-natural grasslands on recently, mid-term and long-term abandoned agricultural fields.**

Spearman-rank correlations of the relative abundances of all individual species combinations between two groups were calculated. The proportion of correlations  $> 0.9$  was divided by the total number of possible interactions to obtain the interaction strength between two groups of species. Line width is proportional to the absolute number of correlations  $> 0.9$ . Line colour and transparency is proportional to the interaction strength, as indicated in the legend in the figure. The size of the circles is proportional to the number of species/taxa in that group. Red filled circles are bacterial groups, blue filled circles are fungal groups. Filled circles of other colours represent other taxa, with identities shown on the figure.

Abbreviations: H.=Herbivorous; R.F.=Root-feeding; S.=Saprotrophic; F.=Fungivorous  
B.=Bacterivorous; H.F.=Herbofungivorous; N.=Nematophagous; O.= Omnivorous;  
O.C.=Omni-carnivorous; P.=Predaceous.

### **Figure 2. Carbon flow in relation to biomass and abundance in the soil food web**

Labelled carbon derived from living components in the soil: roots (green), bacterial channel (red, orange and pink), fungal channel (blue, purple, magenta), and higher trophic levels (brown, yellow, orange). The groups indicated with + represent the amount of  $^{13}\text{C}$  excess in pmol per gram soil (bacteria, fungi, AMF) measured one day after pulse labelling. For all other groups the  $^{13}\text{C}$  excess is the increase in  $\delta^{13}\text{C}$  values of the labelled compared to natural values, measured from non-labelled controls, in recently, mid-term and long-term abandoned agricultural fields. Labelled compounds in plant roots have been measured one day after pulse labelling. Labels in root-feeding nematodes, bacterivorous nematodes, enchytraeids, earthworms, collembolans, fungivorous cryptostigmatic mites and fungivorous nematodes have been determined one week after pulse labelling, and fungivorous non-cryptostigmatic mites, predaceous mites, spiders and omni-carnivorous nematodes were determined two weeks after pulse labelling.

### **Figure 3. Amount of carbon in soil food web components in restored grasslands**

At day 1 the carbon is distributed among microbes. We have therefore presented the relative distribution of carbon scaled to the total amount of labelled carbon in the roots as excess  $^{13}\text{C}$  (the increase in atom% C values of the labelled compared to natural values measured from non-labelled controls) (bacteria, fungi, AMF). The total amount of labelled carbon in the roots decreases during succession (Supplementary Fig 11): Bacteria (red), Fungi (blue) and AMF (light blue) receive carbon from the plant roots. This carbon is distributed into the fungal channel and bacterial channel, where after one week it is taken up by fungivorous mites, nematodes, collembola, and bacterivorous nematodes and earthworms scaled to the total amount of labelled carbon in the roots as excess  $^{13}\text{C}$ . After two weeks the carbon had reached the predators: spiders (brown), predaceous mites (orange) and omnivorous nematodes (yellow). Values of labels in the predators were also scaled to the total amount of labelled carbon in the roots as excess  $^{13}\text{C}$ . Absolute values for these groups are shown in Fig. 2. Abbreviations: F.=Fungivorous; B.=Bacterivorous; P.=Predaceous; O.=Omnivorous.

## Supplementary Tables

Supplementary Table 1

Description of field sites coordinates and time since abandonment.

Field name	Geocoordinates	Abandoned since
Oud Reemst (OR)	N 52°2'27 E 5°48'34	2005
Reijerskamp (REY)	N 52°1'0 E 5°46'21	2005
Telefoonweg (TW)	N 52°00'9 E 5°45'8	2002
De Mossel (MO)	N 52°3'40 E 5°45'8	1995
Nieuw Reemst (NR)	N 52°2'33 E 5°46'29	1990
Wolfhezer Veld (WV)	N 51°59'43 E 5°47'24	1988
Mosselse Veld (MV)	N 52°4'23 E 5°44'13	1985
Dennenkamp (DK)	N 52°1'43 E 5°48'2	1982
Boersbos (BB)	N 52°3'44 E 5°59'57	1982

Supplementary Table 2

Number of taxa within sub-group in each stage of abandonment (occurrence > 1 sample), for recent, mid-term and long-term abandoned fields, used in the Spearman correlation interaction strength network visualization (Fig. 1A)

Nr. Names	Recent	Mid-term	Long-term	Nr. Names	Recent	Mid-term	Long-term
1 Proteobacteria	398	403	346	31 AMF	17	22	30
2 Chloroflexi	54	69	51	32 Ascomycota	70	86	70
3 Actinobacteria	280	241	230	33 Basidiomycota	7	8	9
4 Firmicutes	38	47	34	34 Chytridiomycota	5	2	0
5 Acidobacteria	254	213	245	35 Endophytes	11	10	13
6 Verrucomicrobia	4	99	3	36 Molds	17	41	27
7 Gemmatimonadetes	40	35	36	37 Ectomycorrhiza	5	2	7
8 Nitrospirae	12	5	15	38 Nematophagous fungi	3	9	7
9 Unclassified (bacteria)	258	274	214	39 Other (fungi)	15	17	13
10 Bacteroidetes	64	91	44	40 Potential plant-pathogen	10	14	9
11 WD272	6	7	8	41 Saprotrophic fungi	30	36	31
12 Candidate_division_WS3	11	4	6	42 Unknown fungi	128	136	106
13 Planctomycetes	30	104	39	43 Wood decomposer or parasite	8	9	5
14 Candidate_division_TM7	10	12	6	44 Yeasts	13	14	13
15 Fibrobacteres	3	1	3	45 Zygomycota	4	3	8
16 SHA-109	2	2	0	46 Predaceous mesostigmata	10	14	16
17 Elusimicrobia	1	1	2	47 Herbo-fungivorous cryptostigmata	3	3	3
18 WCHB1-60	1	2	1	48 Predaceous prostigmata	0	3	5
19 Thermotogae	0	0	1	49 Fungivorous cryptostigmata	3	7	10
20 Cyanobacteria	0	2	0	50 Omnivorous prostigmata	1	1	1
21 Chlamydiae	0	3	0	51 Bacterivorous astigmata	0	1	0
22 Armatimonadetes	1	2	1	52 Herbivorous prostigmata	4	4	4
23 Chlorobi	0	1	0	53 Herbivorous cryptostigmata	0	1	2
24 TM6	0	1	1	54 Fungivorous prostigmata	2	3	2
25 SM2F11	0	0	0	55 Fungivorous astigmata	0	1	0
26 Archaea	54	54	54	56 Root-feeding nematodes	6	7	10
27 Fungivorous collembola	12	12	12	57 Bacterivorous nematodes	11	11	13
28 Predaceous collembola	2	2	1	58 Fungivorous nematodes	3	4	3
29 Earthworms	2	2	2	59 Omni-carnivorous nematodes	10	8	10
30 Enchytraeids	15	18	20	60 Plants	29	29	24

Supplementary Table 3

Number of taxa within main group in each stage of abandonment (occurrence > 1 sample), for recent, mid-term and long-term abandoned fields, used in the Spearman correlation interaction strength network visualization (Fig. 1B).

<b>Nr.</b>	<b>Names</b>	<b>Recent</b>	<b>Mid-term</b>	<b>Long-term</b>
1	Bacteria	1467	1620	1286
2	Archaea	54	54	54
3	Collembola	14	14	13
4	Earthworms	2	2	2
5	Enchytraeids	15	18	20
6	AMF	17	22	30
7	Fungi	326	387	318
8	Predaceous mites	10	17	21
9	Fungivorous cryptostigmatic mites	3	7	10
10	Omnivorous mites	4	5	4
11	Herbivorous mites	4	5	6
12	Fungivorous non-cryptostigmatic mites	2	4	2
13	Root-feeding nematodes	6	7	10
14	Bacterivorous nematodes	11	11	13
15	Fungivorous nematodes	3	4	3
16	Omni-carnivorous nematodes	10	8	10
17	Plants	29	29	24
	<b>Subtotals</b>	<b>1977</b>	<b>2214</b>	<b>1826</b>

Supplementary Table 4

Amount of variation explained by all measured soil properties via constrained analysis, which was either linear (RDA) or unimodal (CCA) dependent on the length of the gradient. Then via a forward selection procedure the most explaining soil properties were selected and used to re-analyse the constrained analysis. The variation explained by each of the significant contributing soil properties is displayed below. Phosphorus (P<sub>2</sub>O<sub>5</sub>) is measured as P-Olsen in g/kg, Cation Exchange Capacity (Cobaltihexamine) and all ions indicated with a '+' are measured as cmol+/kg, Residual water content is the g/kg water remaining after drying at 105°C, metals have mg/kg as a unit, Organic Matter, Organic Carbon and Total N are measured as g/kg.

Group	% var. expl. by all soil properties	Most expl. soil property 1			Most expl. soil property 2			Most expl. soil property 3			Most expl. soil property 4			Most expl. soil property 5			Most expl. soil property 6		
		Env. Var.	Var. expl.	P	Env. Var.	Var. expl.	P	Env. Var.	Var. expl.	P	Env. Var.	Var. expl.	P	Env. Var.	Var. expl.	P	Env. Var.	Var. expl.	P
Bacteria	38.9% (CCA)	Fe <sup>+</sup>	10.5%	0.002	Water	6.7%	0.002	Fe	6%	0.002	CEC	5.8%	0.01						
Archaea	46.1% (RDA)	Cu	12.4%	0.042															
Fungi (incl. AMF)	38.4% (CCA)	Fe <sup>+</sup>	10.9%	0.002	C/N	6.2%	0.002	Fe	5.7%	0.006	P	5.3	0.036	pH	5.4%	0.022			
Protists	28.4% (CCA)	Fe <sup>+</sup>	17.1%	0.002	Fe	7.9%	0.004	Cu	7.3%	0.004	P	6.1%	0.004						
Nematodes	34.6% (RDA)	Na <sup>+</sup>	12.6%	0.004	Org. C	7%	0.062	Mg <sup>+</sup>	7.1%	0.013	Ca <sup>+</sup>	9.5%	0.036						
Enchytraeids	54.4% (CCA)	Fe <sup>+</sup>	17%	0.002	Fe	7.9%	0.004	Cu	7.3%	0.004	P	6.1%	0.01	Org C	6.4%	0.004	Ca	5.0%	0.038
Mites	29.4% (RDA)	P	13%	0.016	Al <sup>+</sup>	12.3%	0.018												
Collembola	48.5% (RDA)	Fe <sup>+</sup>	16.6%	0.024	K <sup>+</sup>	11.5%	0.05	C/N	14.4%	0.028									
Plants	68.4% (CCA)	pH	13.2%	0.002	Org. C	11.1%	0.002	P	7.9%	0.008	Al <sup>+</sup>	6.8%	0.002	C/N	6.9%	0.006	Tot N	6.9%	0.002

Supplementary Table 5:

Nested ANOVA results for each of the graphs from Supplementary Fig. 4. We analysed the number of species per aggregated group in three ways: the effect of site, succession, and time since abandonment. The sites OR, REY and TW (S-Table 1) were categorized as recently abandoned fields, MO, NR and WV as mid-term abandoned fields and MV, DK and BB as long-term abandoned fields. These categories mark the factor 'succession'. We also analysed the effect as a regression taking 'time since abandonment' as a continuous variable (S-Table 1). For the other factors we used a nested ANOVA approach: when testing 'site' as a factor, subplots were nested in 'site' and when testing 'succession' as a factor, sites were nested in 'succession'.

	Site		Succession		Time since abandonment	
	<i>F-values</i>	<i>P-values</i>	<i>F-values</i>	<i>P-values</i>	<i>F-values</i>	<i>P-values</i>
Bacteria	12.4	<b>&lt;0.0001</b>	44.4	<b>&lt;0.0001</b>	1.28	0.274
Archaea	1.11	0.412	0.348	0.712	1.06	0.316
Collembola	1.03	0.449	0.225	0.801	<0.001	0.984
Earthworms	1.96	0.112	1.86	0.185	<0.001	0.978
Enchytraeids	0.407	0.902	0.215	0.808	0.399	0.536
AMF	1.85	0.136	2.71	0.095	5.93	<b>0.026</b>
Fungi	1.3	<b>&lt;0.0001</b>	33.8	<b>&lt;0.0001</b>	0.156	0.698
Predaceous mites	2.2	0.078	7.51	<b>0.0043</b>	14.4	<b>0.001</b>
Fungivorous cryptostigmatic mites	8.82	<b>&lt;0.0001</b>	14.4	<b>&lt;0.001</b>	36.3	<b>&lt;0.0001</b>
Omnivorous mites	0.763	0.639	0.684	0.517	1.58	0.225
Herbivorous mites	6.38	<b>&lt;0.001</b>	9.75	<b>0.0014</b>	27.3	<b>&lt;0.0001</b>
Fungivorous non-cryptostigmatic mites	1.4	0.262	1.4	0.272	0.072	0.792
Root-feeding nematodes	4.85	<b>0.003</b>	10.7	<b>&lt;0.001</b>	10.5	<b>0.005</b>
Bacterivorous nematodes	2.52	<b>0.049</b>	4.84	<b>0.021</b>	9.07	<b>0.007</b>
Fungivorous nematodes	4.67	<b>0.003</b>	1.17	0.334	1.98	0.176
Omni-carnivorous nematodes	1.02	0.458	0.557	0.583	0.173	0.683
Plants	9.48	<b>&lt;0.0001</b>	11.3	<b>&lt;0.001</b>	31.4	<b>&lt;0.0001</b>
Ectomycorrhiza	2.6	<b>0.047</b>	4.95	<b>0.02</b>	0.144	0.709
Predaceous mesostigmata	2.06	0.096	5.48	<b>0.014</b>	9.54	<b>0.006</b>

Supplementary Table 6:

Connectance calculated for the networks in Fig. 1. For recent- mid-term- and long-term abandonment all correlations > 0.9 (represented in Fig. 1, main text) divided by all possible connections between the members of the nodes.

sub-groups	Recent	Mid-term	Long-term		main groups	Recent	Mid-term	Long-term
correlations > 0.9	10961	26571	19308		correlations > 0.9	4833	12621	9029
all possible correlations	1749816	2239795	1510742		all possible correlations	822361	1057646	786379
connectance %	0.626	1.186	1.278		connectance %	0.588	1.193	1.148

Supplementary Table 7:

PERMANOVA results on changes in community composition of plants, archaea, bacteria, fungi, protists, nematodes, enchytraeids, collembolan, mites and earthworms. In case of clear differences between abundance data and present-absence data, an additional ANOSIM analysis was performed. Significant p-values are marked in bold. Most groups did change in community assemblage over successional stage.

PERMANOVA on abundance data	Total SS	Within group SS	F	p	sig. Difference between groups			ANOSIM on presence-absence data				sig. Difference between groups		
					recent-mid-term	recent-long-term	mid-term-long-term	Mean rank within	Mean rank between	R	p	recent-mid-term	recent-long-term	mid-term-long-term
Plants	4,71E+04	3,65E+04	3.486	<b>0.0015</b>	no	yes	yes	146.5	189.1	0.2425	<b>0.0009</b>	yes	yes	no
Archaea (TRFLP data)	2.413	1.765	3.855	<b>0.0084</b>	yes	yes	no							
Bacteria	6,98E+05	5,79E+05	2.365	<b>0.0063</b>	yes	no	no	123.6	180.5	0.3499	<b>0.0001</b>	yes	no	yes
Fungi	1,34E+05	1,10E+05	2.581	<b>0.0001</b>	yes	yes	yes	116.3	183.8	0.4156	<b>0.0001</b>	yes	yes	yes
Protists	2,79E+08	2,27E+08	0.8014	0.6118	no	no	no							
Nematodes	2,32E+08	2,19E+08	0.7375	0.7857	no	no	no	145.2	189.7	0.2532	<b>0.0009</b>	no	yes	no
Enchytraeids	2,34E+05	2,11E+05	1.303	0.1336	no	yes	no	150.8	187.2	0.2076	<b>0.0004</b>	yes	yes	yes
Collembola	5,49E+04	4,93E+04	1.377	0.2277	no	no	no	174.4	176.7	0.01288	0.3532	no	no	no
Mites	7,55E+10	7,04E+10	0.881	0.5871	no	no	no	141.3	191.4	0.2855	<b>0.0005</b>	yes	yes	no
Earthworms	170.6	153.6	1.331	0.2673	no	no	no							



## Supplementary Table 8

Average label in each of the measured groups at all harvest points: 1 day, 1 week and 2 weeks after pulse labelling in atom% C. The table shows the significance levels of the three successional stages in an ANOVA with a nested design. The sites OR, REY and TW (S-Table 1) were categorized as recently abandoned fields, MO, NR and WV as mid-term abandoned fields and MV, DK and BB as long-term abandoned fields. These categories mark the factor 'succession'. Where sites are nested in succession time.

Generalized Linear Model with Nested design. Field nested in succession time

			Average	Stdev	Stats
<b>1 day</b>	Plant shoots	Recent	1.62	0.334	$F_{(2,17)} = 0.18$ , $p=0.83$
		Mid	1039,00	0.482	
		Long	1098,00	0.363	
	Plant roots	Recent	0.119	0.086	$F_{(2,15)} = 0.42$ , $p=0.67$
		Mid	0.080	0.052	
		Long	0.038	0.017	
	Soil	Recent	0.000	0.000	$F_{(2,16)} = 2.49$ , $p=0.11$
		Mid	0.001	0.001	
		Long	0.000	0.000	
<b>1 week</b>	Earthworms	Recent	0.008	0.005	$F_{(2,5)} = 0.70$ , $p=0.54$
		Mid	0.001	0.000	
		Long	0.003	nd	
	Root-feeding nematodes	Recent	0.175	0.062	$F_{(2,14)} = 0.20$ , $p=0.82$
		Mid	0.164	0.072	
		Long	0.157	0.055	
	Fungal-feeding nematodes	Recent	0.045	0.040	$F_{(2,6)} = 0.35$ , $p=0.72$
		Mid	0.003	0.004	
		Long	0.009	0.003	
	Fungivorous collembola	Recent	0.125	0.056	$F_{(2,15)} = 2.54$ , $p=0.11$
		Mid	0.204	0.107	
		Long	0.011	0.010	
	Fungivorous cryptostigmatic mites	Recent	0.007	0.004	<b><math>F_{(2,8)} = 6.62</math></b> , <b><math>p=0.02</math></b>
		Mid	0.056	0.067	
		Long	0.025	0.022	
	Fungivorous prostigmatic mites	Recent	0.000	0.000	<b><math>F_{(4,5)} = 9.42</math></b> , <b><math>p=0.02</math></b>
		Mid	0.012	0.010	
		Long	0.001	0.001	
	Herbivorous bugs	Recent	0.340	0.233	$F_{(1,6)} = 0.48$ , $p=0.52$
		Mid	0.293	0.131	
		Long	nd	nd	
<b>2 weeks</b>	Bacterial feeding nematodes	Recent	0.009	0.003	$F_{(2,16)} = 2.16$ , $p=0.15$
		Mid	0.013	0.007	
		Long	0.021	0.008	
	Fungivorous astigmatic mites	Recent	0.004	0.003	<b><math>F_{(2,6)} = 5.79</math></b> , <b><math>p=0.04</math></b>
		Mid	0.013	0.012	
		Long	0.005	0.002	
	Predaceous mites	Recent	0.008	0.007	$F_{(2,38)} = 0.79$ , $p=0.46$
		Mid	0.01	0.006	
		Long	0.059	0.085	
	Predaceous spiders	Recent	0.126	0.012	$F_{(2,10)} = 0.56$ , $p=0.59$
		Mid	0.216	0.035	
		Long	0.177	nd	
	Omnivorous nematodes	Recent	0.014	0.006	$F_{(2,18)} = 0.90$ , $p=0.43$
		Mid	0.026	0.009	
		Long	0.016	0.008	

## Supplementary Table 9

Averages and standard deviations of delta  $^{13}\text{C}$  values of unlabelled controls and labelled material of 1 day, 1 week and two weeks after pulse labelling. Numbers in bold indicate the highest numbers, the moment at which the pulse has in

incorporated most  $^{13}\text{C}$  in the tissue of the measured group of soil biota. That point was chosen to represent the label incorporated in that specific group of soil organisms

	Non-labeled		1 day		1 week		2 weeks	
	Average	Stdev	Average	Stdev	Average	Stdev	Average	Stdev
Plant shoots	-29.54	1.28	<b>1002.33</b>	<b>713.03</b>	959.07	363.87	563.79	358.55
Plant roots	-29.78	0.57	<b>42.65</b>	<b>108.56</b>	23.42	72.20	53.36	99.01
Soil	-27.92	0.96	<b>-27.42</b>	<b>1.18</b>	-27.54	1.45	-27.08	1.38
Earthworms	-25.82	1.12	-22.94	6.60	<b>-22.72</b>	<b>5.31</b>	-22.07	3.38
Root-feeding nematodes	-27.43	5.78	80.54	96.50	<b>125.39</b>	<b>111.64</b>	125.95	172.38
Fungal-feeding nematodes	-27.94	2.35	-25.47	3.10	<b>-7.33</b>	<b>49.83</b>	-9.42	25.23
Fungivorous collembola	-23.42	1.84	57.19	62.80	<b>93.05</b>	<b>149.33</b>	81.15	106.62
Fungivorous cryptostigmatic mites	-24.63	0.27	-17.22	15.17	<b>-11.72</b>	<b>27.60</b>	-20.58	6.00
Fungivorous prostigmatic mites	-23.99	0.32	-16.20	13.21	<b>-18.68</b>	<b>13.20</b>	-19.34	8.14
Herbivorous bugs	-21.65	-	<b>541.14</b>	<b>963.12</b>	294.63	358.55	135.46	130.44
Bacterial feeding nematodes	-26.66	2.59	-16.60	27.08	-19.68	7.18	<b>-15.11</b>	<b>11827.00</b>
Fungivorous astigmatic mites	-22.45	3.76	-22.94	4.47	-23.03	3.73	<b>-17.38</b>	<b>13.47</b>
Predaceous mites	-23.84	2.52	-16.65	9.22	-14.31	18.28	<b>-1.66</b>	<b>86.77</b>
Predaceous spiders	-24.21	1.82	-24.83	1.72	167.54	262.84	<b>125.70</b>	<b>76.11</b>
Omnivorous nematodes	-24.06	9.11	-20.71	9.32	-1.656	36.39	<b>-6.84</b>	<b>14.56</b>
Enchytraeds	-27.67	-	-17.21	10.78	-39.79	-	-28.94	5.12

## Supplementary Figures

### Supplementary Figure 1

Map of sampling sites in The Netherlands

### Supplementary Figure 2

Venn-diagram showing the overlap in species occurrence of the 3553 species/taxa that were included in the network analysis. Number of species/taxa in recent- (blue), mid-term- (red) and long-term abandoned soils (green). Numbers represented in single circle represent the number of species/taxa that are specifically found in that stage of abandonment. Numbers represented in the overlap of two circles represent species/taxa that occur in both these stages of abandonment, and the number in the overlap of the three circles represent species/taxa that occur in all abandonment stages.

### Supplementary Figure 3

Principal Component Analysis of site variation explained by the physiochemical data collected in October 2011. Abbreviations of field sites have been provided in the site description of Supplementary Table 4. Phosphorus ( $P_2O_5$ ) is measured as P-Olsen in g/kg, Cation Exchange Capacity (Cobaltihexamine) and all ions indicated with a '+' are measured as cmol/kg, Residual water content is the g/kg water remaining after drying at 105°C, metals have mg/kg as a unit, Organic Matter, Organic Carbon and Total N are measured as g/kg.

### Supplementary Figure 4

Graphical representation of the Supplementary Table 5 showing number of taxa in each stage of abandonment per sampling site. Abbreviations of field sites see site description Supplementary Table 1. Additional to Supplementary Table 5 the ectomycorrhizal fungi and predaceous mesostigmata are displayed since they show significant patterns along the successional gradient. Total amount of species within the different species groups were plotted among field sites (each bar), categories of sites (recent- (blue), mid- (red) and long-term (green) abandoned) and in years since abandonment (left to right). Abbreviations: E. M. fungi=Ectomycorrhizal fungi, F. C. mites=Fungivorous cryptostigmatic mites, P. mesostigmata=Predaceous mesostigmatic mites, R.F. nematodes=Root-feeding nematodes, B. nematodes=Bacterivorous nematodes, OC. nematodes=Omni-carnivorous nematodes, F. nematodes=Fungivorous nematodes, P. mites= Predaceous mites, F.NC. Mites=Fungivorous non-cryptostigmatic mites, O. mites=Omnivorous mites H. mites=Herbivorous mites.

### Supplementary Figure 5

A. Average H-values of recent, mid-term and long-term plant communities. B. Principal coordinate analysis (PCO) on presence-absence data of the plant species in the field sites. Statistical summary on the difference between recent, mid-term and long-term sites is presented in Supplementary Table 7 under ANOSIM analysis of the plant community in the field sites where the experimental cores were extracted.

### Supplementary Figure 6

Non-metric Multidimensional Scaling (NMDS) of the rank abundance of the three most dominated plant species (*Agrostis capillaris*, *Holcus lanatus*, *Plantago lanceolata*) in each of the experimental cores, which shows strong overlap in the plant community between the cores.

### Supplementary Figure 7

A. Shoot + root biomass in grams of the plants from the cores at the time of harvest. Abbreviations of field sites see site description Supplementary Table 1. B. C/N ratio of the plant shoots and roots from the cores at the time of harvest. Abbreviations of field sites see site description Supplementary Table 1.

### Supplementary Figure 8

Network visualisation of the interaction strengths between the species sub-groups in recently, mid-term and long-term abandoned agricultural fields. Spearman correlations between the co-occurrences of all individual species of different fields were calculated. The proportion of correlations > 0.9 was divided by the total number of possible interactions in order to obtain the interaction strength between two groups of species. Line width is proportional to the absolute number of correlations > 0.9. Line colour and transparency is proportional to the interactions strength as indicated in the legend. The size of the circles is proportional to the number of species/taxa in that group. Red circles are bacterial groups, blue circles are fungal groups. Abbreviations: H.=Herbivorous R.F.=Root-feeding S.=Saprotrophic F.=Fungivorous B.=Bacterivorous H.F.=Herbofungivorous N.=Nematophagous O.=Omnivorous O.C.=Omni-carnivorous P.=Predaceous.

### Supplementary Figure 9

Network visualisation of the interaction strengths between the main species groups in recently, mid-term and long-term abandoned agricultural fields. Spearman correlations between the co-occurrence of all individual species of different fields were calculated. The proportion of correlations > 0.9 was divided by the total number of possible interactions to obtain the interaction strength between two groups of species. Line width is proportional to the absolute number of correlations > 0.9. Line colour and transparency is proportional to the interactions strength as indicated in the legend. The size of the circles is proportional to the number of species/taxa in that group. Red circles are bacterial groups, blue circles are fungal groups. Abbreviations: H.=Herbivorous R.F.=Root-feeding S.=Saprotrophic F.=Fungivorous B.=Bacterivorous H.F.=Herbofungivorous N.=Nematophagous O.=Omnivorous O.C.=Omni-carnivorous P.=Predaceous.

#### Supplementary Figure 10

Results of ANOSIM (Euclidian) analyses on soil properties at recent, mid- and long-term abandoned fields. The variation of the similarities between groups (recent-, mid-term-, long-term abandoned since agricultural practice, first boxplot left) is larger than the variation within groups 1, 2 and 3 representing recent-, mid-term and long-term abandonment ( $R=0.2333$ ;  $p=0.0041$ ). Within groups the variation of the recently abandoned fields is significantly higher than of the mid-term abandoned fields ( $p=0.0033$ ), however, not significantly higher than of the long-term abandoned fields ( $p=0.0544$ ).

#### Supplementary Figure 11

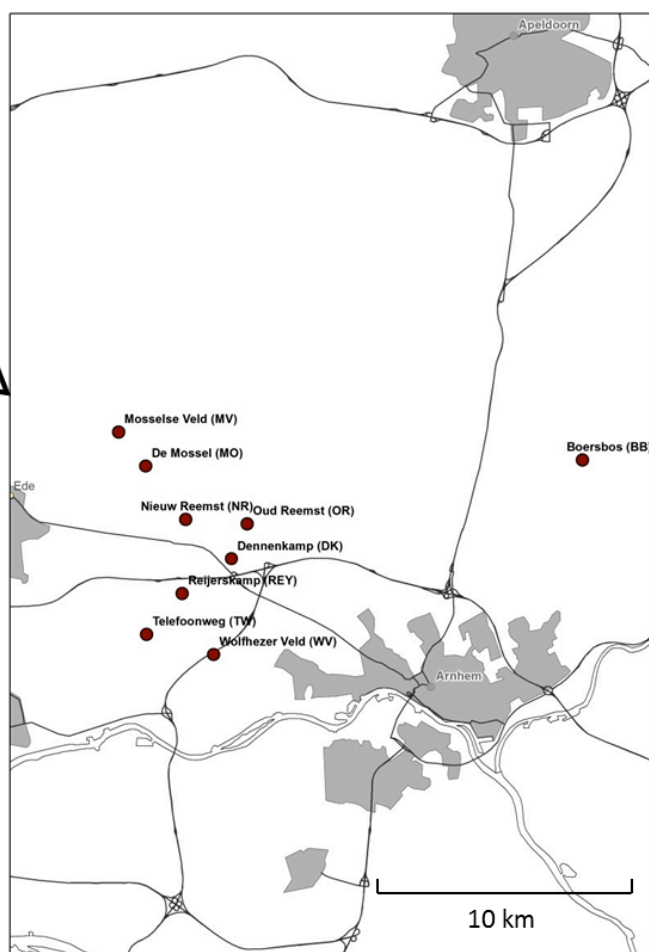
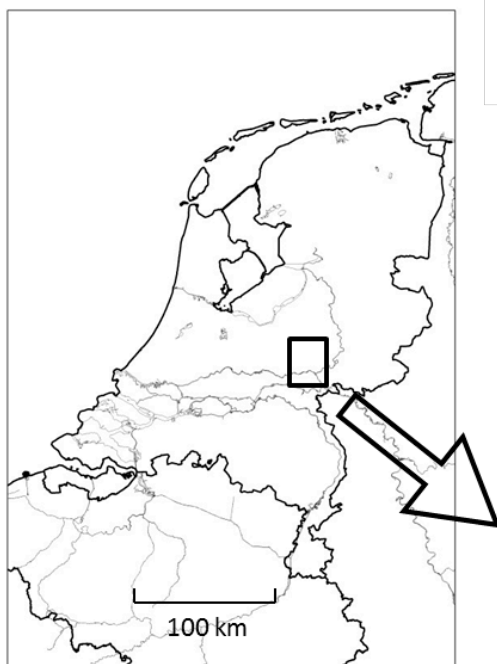
Fungal (F) to bacteria (B) ratios in the three abandonment stages; left panel F to B ratio of excess C (labelled excess in contrast to unlabelled controls) in phospholipid fatty acids (PLFA). Right panel the total F to B ratios in PLFAs.

#### Supplementary Figure 12

Carbon and nitrogen flow in the soil food-web during 2 weeks. The root derived carbon is marked with grey, shoot carbon with green, bacterial-based channel with red, fungal-based channel with blue and the higher trophic level interactions with purple and pink. The plots with standard deviation represent the amount of  $^{13}\text{C}$  excess in pmol per gram soil (bacteria, fungi, AMF), or  $\delta^{13}\text{C}$  and  $\delta^{15}\text{N}$  excess (all other groups) compared to natural values measured from non-labelled controls in recently (light grey), mid-term (dark grey) and long-term (black) abandoned agricultural fields. The statistical analyses of the treatment effects with field site as a factor nested in successional stage are presented in boxes next to the figure. The darker coloured arrows depict the carbon flow in the food web while the lighter coloured (dashed) arrows depict the nitrogen flow. The width of the arrows between groups reflects the percentage of correlation  $>0.9$  between groups in all the fields as in Fig. 1. The pie charts above the arrows are also calculated from Fig. 1, and represent the proportion of significant interactions in recently (light grey), mid-term (dark grey) and long-term (black) abandoned fields. The  $(\rho)p$  values at the arrows represent the Spearman-rank correlation values between the groups that are connected by the arrow, which is calculated from the labelling data. Significant correlations are bold and marked with darker arrow colour. By correlation analysis of pulse labelling data we wanted to analyse the potential of feeding relationships that emerged on the basis of correlations in the network analysis.

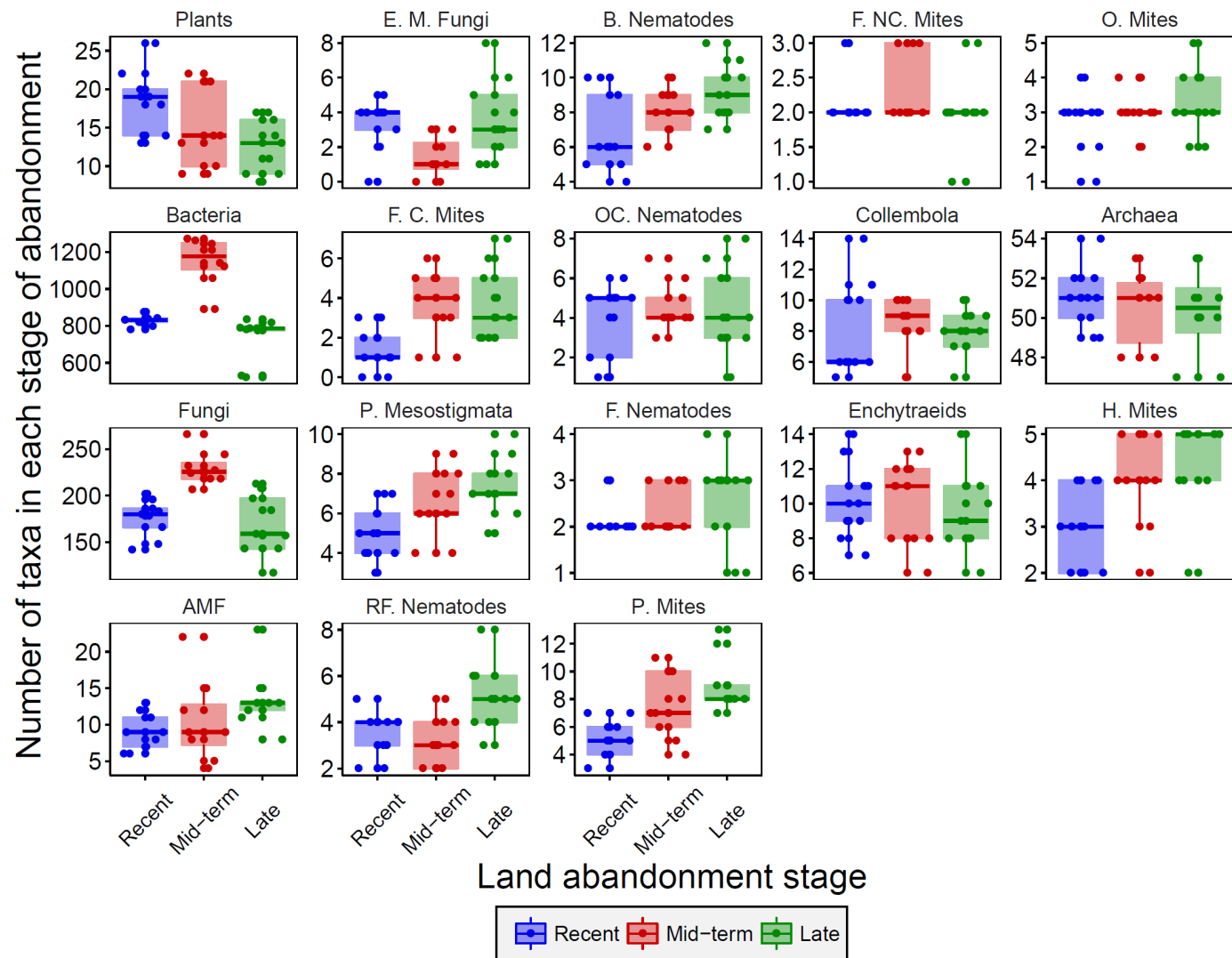
#### Supplementary Figure 13

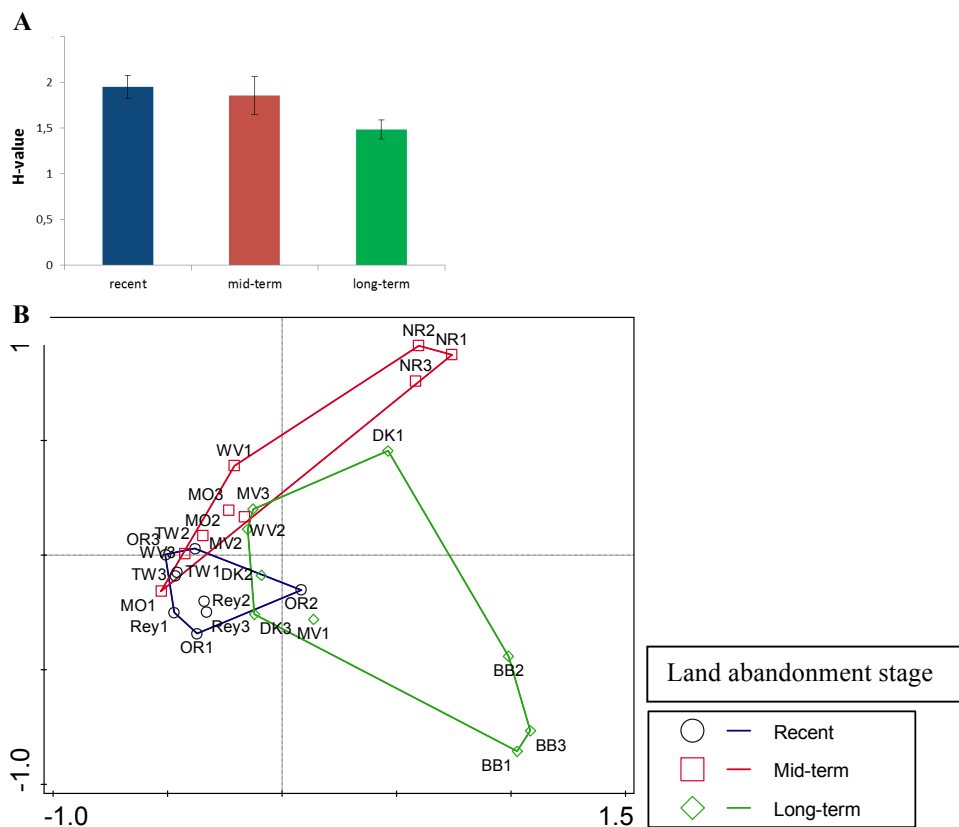
Core harvesting scheme



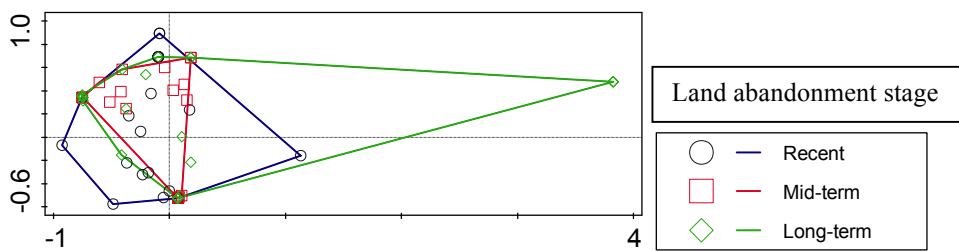
Supplementary Figure 1



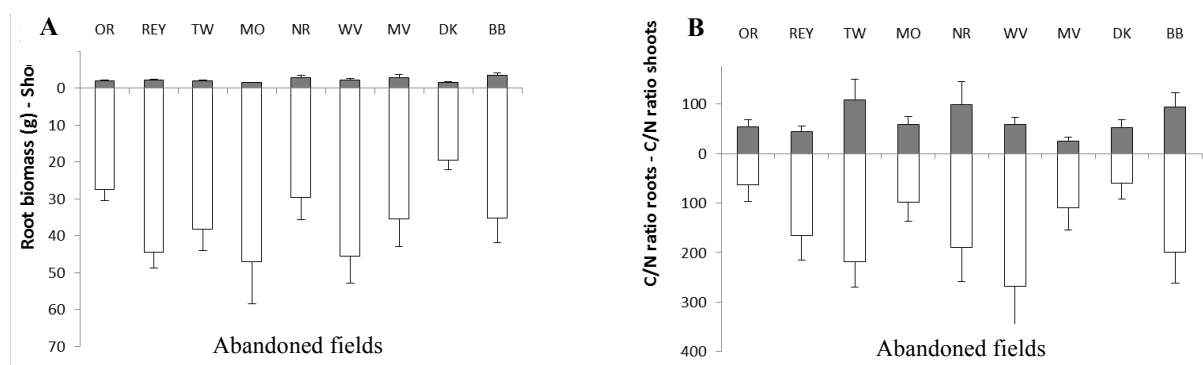




Supplementary Figure 5



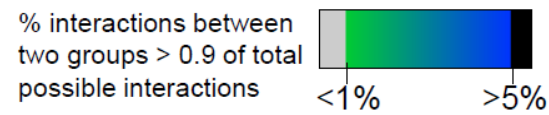
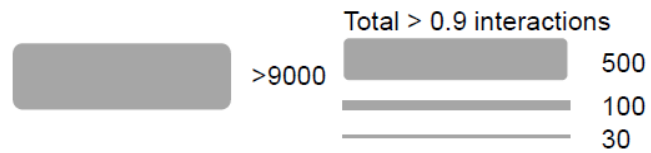
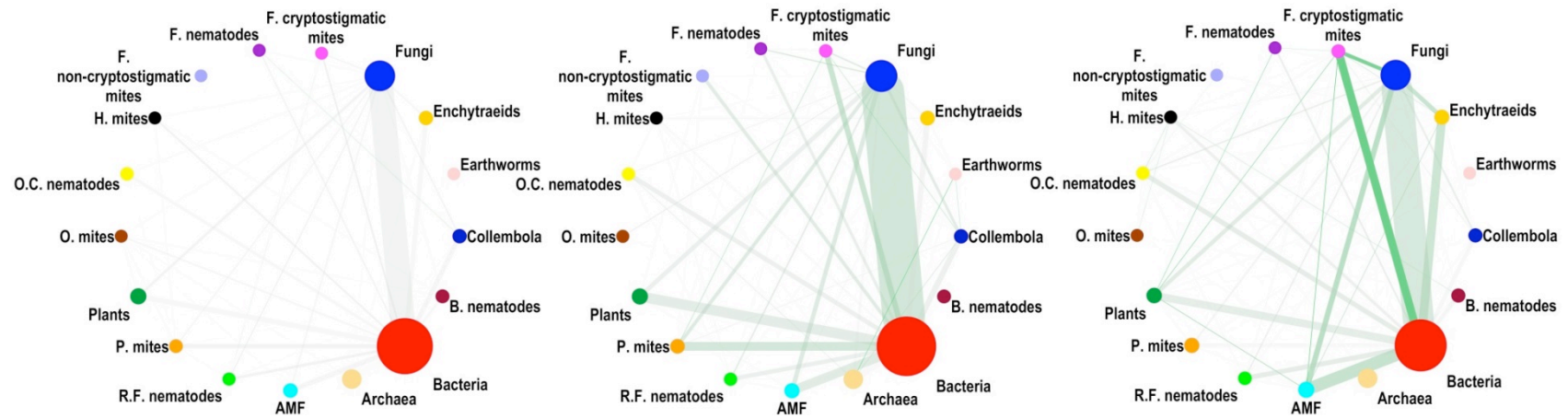
Supplementary Figure 6



Supplementary Figure 7

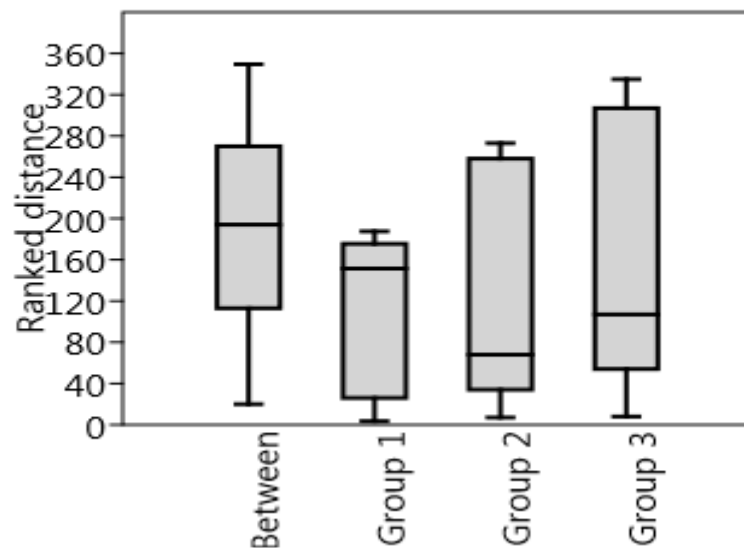




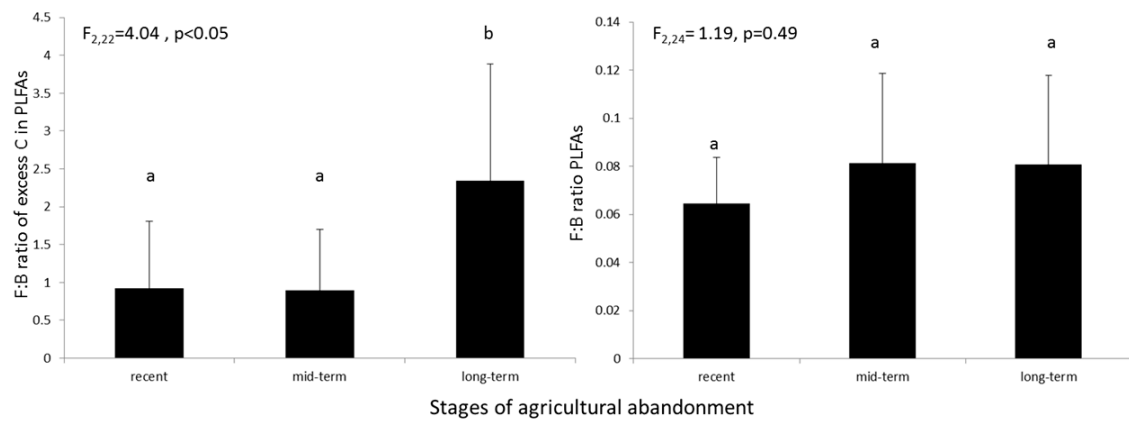


Supplementary Figure 9

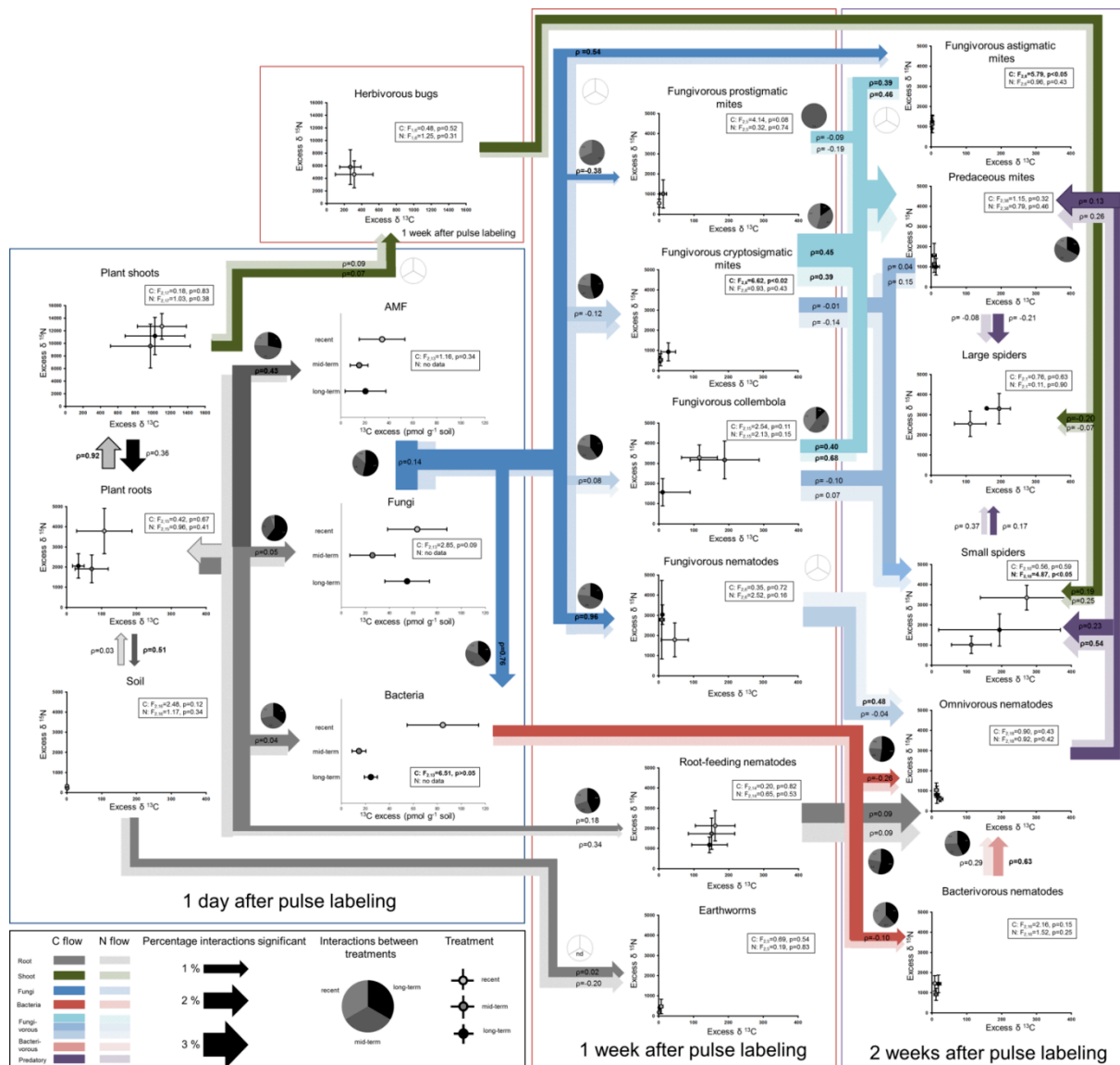




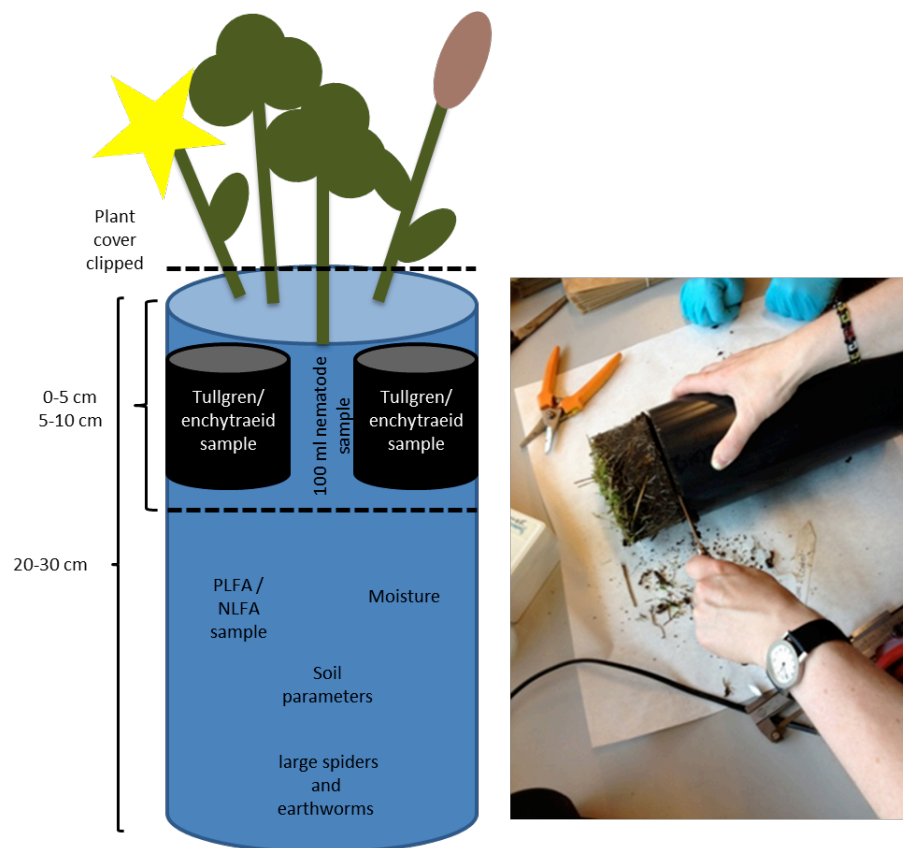
Supplementary Figure 10



Supplementary Figure 11



Supplementary Figure 12



Supplementary Figure 13

